

# Methane bubbling from Siberian thaw lakes as a positive feedback to climate warming

K. M. Walter<sup>1</sup>, S. A. Zimov<sup>2</sup>, J. P. Chanton<sup>3</sup>, D. Verbyla<sup>4</sup> & F. S. Chapin III<sup>1</sup>

Large uncertainties in the budget of atmospheric methane, an important greenhouse gas, limit the accuracy of climate change projections<sup>1,2</sup>. Thaw lakes in North Siberia are known to emit methane<sup>3</sup>, but the magnitude of these emissions remains uncertain because most methane is released through ebullition (bubbling), which is spatially and temporally variable. Here we report a new method of measuring ebullition and use it to quantify methane emissions from two thaw lakes in North Siberia. We show that ebullition accounts for 95 per cent of methane emissions from these lakes, and that methane flux from thaw lakes in our study region may be five times higher than previously estimated<sup>3</sup>. Extrapolation of these fluxes indicates that thaw lakes in North Siberia emit 3.8 teragrams of methane per year, which increases present estimates of methane emissions from northern wetlands (<6–40 teragrams per year; refs 1, 2, 4–6) by between 10 and 63 per cent. We find that thawing permafrost along lake margins accounts for most of the methane released from the lakes, and estimate that an expansion of thaw lakes between 1974 and 2000, which was concurrent with regional warming, increased methane emissions in our study region by 58 per cent. Furthermore, the Pleistocene age (35,260–42,900 years) of methane emitted from hotspots along thawing lake margins indicates that this positive feedback to climate warming has led to the release of old carbon stocks previously stored in permafrost.

Understanding the role of North Siberian thaw lakes in the global atmospheric methane (CH<sub>4</sub>) budget is important because the concentration of atmospheric CH<sub>4</sub>, a potent greenhouse gas, is highest at 65° to 70° N (refs 1, 7), has risen during recent decades<sup>1,8</sup>, and exhibits an inexplicably large seasonal amplitude at high northern latitudes with bimodal maxima in winter and spring<sup>7</sup>—times of year when wetlands are frozen, but unfrozen lake sediments actively produce and emit CH<sub>4</sub>. This study shows that ebullition from Siberian thaw lakes is a large and increasing source of atmospheric CH<sub>4</sub> as Siberian thaw lakes continue to expand.

Thaw lakes comprise 90% of the lakes in the Russian permafrost zone<sup>9</sup>. Many North Siberian lakes differ from lakes in America and Europe because they are underlain by yedoma, an organic-rich (~2% carbon by mass) Pleistocene-age loess permafrost with ice content of 50–90% by volume<sup>3,10,11</sup>. Thermokarst erosion occurs along lake margins when massive, subsurface ground ice wedges melt, causing the ground surface to subside. Labile organic matter from permafrost erodes into anaerobic lake bottoms when yedoma thaws, enhancing methane production and emission<sup>3</sup>. In this study we used remote sensing, aerial surveys and year-round, continuous measurements of CH<sub>4</sub> flux to (1) quantify CH<sub>4</sub> emissions from North Siberian lakes, paying particular attention to the role of ebullition, and (2) document the role of thermokarst erosion as a landscape process that fuels CH<sub>4</sub> production and feeds back to climate warming.

Ebullition is often the dominant pathway of CH<sub>4</sub> release from aquatic ecosystems<sup>12,13</sup>, yet it is seldom measured owing to its extreme temporal and spatial patchiness. Siberian lakes provide a unique opportunity to assess ebullition flux more accurately. As ice forms in autumn, bubbles released from lake sediments are frozen in place, allowing accurate mapping of ebullition 'point sources' across lake surfaces (Fig. 1). We used random and selective placement of bubble traps under water or ice to make continuous measurements of 'background' (measured with randomly placed traps), 'point-source' (moderately high bubble flux from discrete points in lake sediments) and 'hotspot' (open holes in ice due to extremely high bubble flux from discrete points in lake sediments) fluxes from April 2003 through May 2004 on two intensively studied lakes in North Siberia.

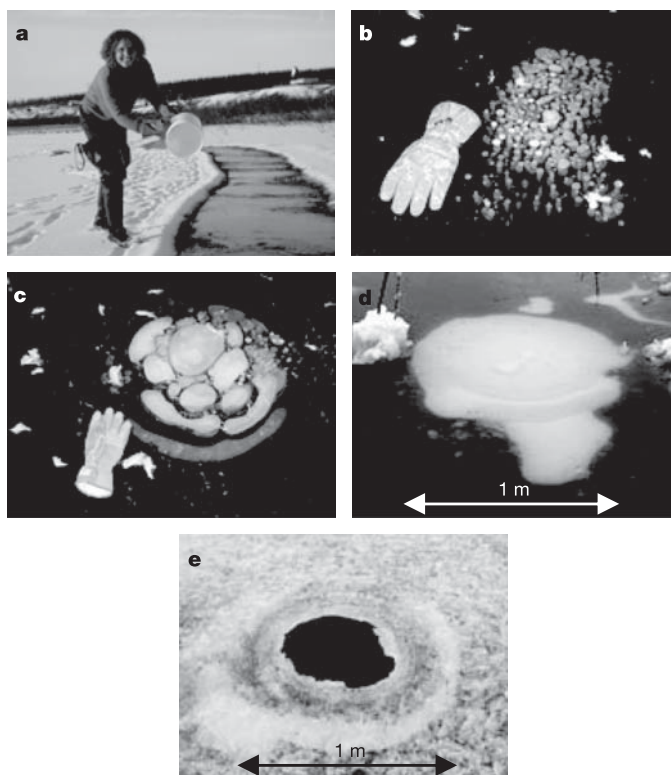


**Figure 1 | Photographs of CH<sub>4</sub> bubbles trapped in lake ice represent point sources of bubbling.** The distribution of ebullition point sources was measured along transects on lake ice (a), recognizing four distinct categories of bubble clusters with associated CH<sub>4</sub> emission rates (Supplementary Information): b, *kotenok*; c, *koshka*; d, *kotara*; e, *hotspot*.

<sup>1</sup>Institute of Arctic Biology, University of Alaska Fairbanks, Alaska 99775, USA. <sup>2</sup>Northeast Science Station, Cherskii 678830, Russia. <sup>3</sup>Department of Oceanography, Florida State University, Florida 32306, USA. <sup>4</sup>Forest Science Department, University of Alaska Fairbanks, Alaska 99775, USA.

**Table 1 | Summary of CH<sub>4</sub> flux components and isotopes in bubbles from North Siberian thermokarst lakes**

Season 2003-04	Flux component	Whole lake (g CH <sub>4</sub> m <sup>-2</sup> yr <sup>-1</sup> )	Percentage of annual flux	Thermokarst margins (g CH <sub>4</sub> m <sup>-2</sup> yr <sup>-1</sup> )	<sup>14</sup> CH <sub>4</sub> age (years)	<sup>14</sup> CH <sub>4</sub> (% modern carbon)	δ <sup>13</sup> C of CH <sub>4</sub> (‰)	δD of CH <sub>4</sub> (‰)
Summer (open water June–September)	Background ebullition	5.7 ± 2.0	22 ± 6	27.7 ± 14	1,345 to 5,350	51–85	–57.7 to –73.7	–420 to –338
	Point source	6.2 ± 0.7	25 ± 5	34.7 ± 0.7	5,590 to 12,285	22–50	–62.6 to –82.8	–388 to –376
	Hotspots	1.0 ± 0.7	4 ± 2	5.4 ± 3.9	35,570 to 39,120	0.77–1.2	–78.5 to –80.4	–401 to –392
	Molecular diffusion	1.3 ± 0.1	5 ± 1	1.3 ± 0.1				
Winter (ice cover October–May)	Background ebullition	0.5 ± 0	2 ± 0	0.7 ± 0				
	Point source	8.3 ± 0.9	34 ± 7	46.9 ± 0.9	22,050	6.4	–76.0 to –78.3	–394 to –379
	Hotspots	2.0 ± 1.3	8 ± 5	11.1 ± 7.7	35,260 to 42,900	0.49–1.2	–71.7 to –80.4	–420 to –388
Total		24.9 ± 2.3	100	127.8 ± 24.0	16,520†			

† Sum of the mean radiocarbon age of each flux component weighted by each component's proportion of total annual emissions. Forty-four per cent of annual CH<sub>4</sub> emissions from Siberian lakes occurs in winter and spring when CH<sub>4</sub> trapped as bubble clusters in lake ice is released to the atmosphere during high temperature anomalies<sup>3</sup>, overflow events when lake water is forced through lenses of ice clusters and open holes after heavy snowfall, and springtime thaw of lake ice<sup>17</sup>. Error estimates are half of the absolute difference between measurements for two intensive study lakes. Sources of variability are shown in Supplementary Table 1.

We extrapolated fluxes regionally using the distribution of hotspots in aerial photographs.

Ebullition comprised 95 ± 1% of the CH<sub>4</sub> flux from the intensively studied lakes, with molecular diffusion contributing the remainder (Table 1). Emergent plants were absent as a conduit in our lakes. Point sources comprised the largest proportion (59 ± 12%) of total CH<sub>4</sub> emissions. Ebullition rates were highest in traps selectively placed over hotspots along thermokarst margins of lakes (Fig. 2), with hotspots <1% of lake area but contributing 11 ± 7% of the total CH<sub>4</sub> flux. The maximum rate of 18,835 mg of CH<sub>4</sub> per day per hotspot (>30 litres per day per hotspot) exceeds most published CH<sub>4</sub> flux rates for lakes and wetlands by several orders of magnitude<sup>4,5,12–17</sup>.

Hotspots were visible as 'black holes' in lake ice along thermokarst margins in ground and aerial surveys of lakes (Supplementary Information). Half of the 60 lakes surveyed in our study region (including our two intensively studied lakes) had modest thermo-

karst erosion, marked by banks with gentle slopes, stable vegetation and hotspots distributed primarily in a 15-m-wide belt along thaw margins. The remaining lakes had more intense thermokarst erosion, with steep muddy banks, occasional exposed ice wedges, and a >30-m-wide belt of hotspot emissions at the lake margins.

When background, point-source, and hotspot ebullition fluxes were aggregated to a whole-lake basis, the annual flux was 24.9 ± 2.3 g CH<sub>4</sub> m<sup>-2</sup> yr<sup>-1</sup> from the intensively studied lakes. Our estimate is conservative because it neglects other extreme expulsions of CH<sub>4</sub> from lakes, which were not measured because of their rarity (Supplementary Information). Fluxes from the 15-m-wide band of active thermokarst on the eroding edge of lakes (15.8% of lake area, 128 ± 24 g CH<sub>4</sub> m<sup>-2</sup> yr<sup>-1</sup>) accounted for 79% of total lake emissions. In the other 50% of the region's lakes, where we extrapolated the thermokarst margin flux to the >30-m-wide band in which hotspots were observed (31.6% of lake area), we estimate that thermokarst margins accounted for 90% of the lake-averaged annual flux of 43.7 ± 3.2 g CH<sub>4</sub> m<sup>-2</sup> yr<sup>-1</sup>.

These emission rates exceed those reported in previous work on the same lakes (6.8 g CH<sub>4</sub> m<sup>-2</sup> yr<sup>-1</sup>; ref. 3), other high-latitude lakes and ponds (0.5–11.3 g CH<sub>4</sub> m<sup>-2</sup> yr<sup>-1</sup>; refs 17–19), and North Siberian wetlands (0.9–14.3 g CH<sub>4</sub> m<sup>-2</sup> yr<sup>-1</sup>; refs 20, 21) and 6.4 ± 3.4 g CH<sub>4</sub> m<sup>-2</sup> yr<sup>-1</sup> (*n* = 8 chambers measured biweekly from June–October in 2003; this study)].

Our lake estimate probably exceeds others not only because of the prevalence of thermokarst activity in North Siberia, but also because our stratified sampling design with continuous measurements and mapping point sources and hotspots accounted for the patchiness of bubbling. The few studies that previously measured ebullition estimated fluxes from a few randomly placed bubble traps that were periodically deployed<sup>13,12,13,22</sup>. In our study, random placement of up to 14 traps per lake with continuous, year-round monitoring revealed that this 'background' bubbling accounted for only 24 ± 6% of the total emissions. To our knowledge, this is the first study to quantify the spatial and temporal patchiness of ebullition in any lake, thereby reducing uncertainty in a highly sporadic mode of methane emission.

We extrapolated our lake flux estimate to the yedoma region of North Siberia using an estimated lake area for the region of 11% as measured in our Geographical Information Systems (GIS) study—which is conservative given the range of lake area estimates for this region (8.5 to >30% of the yedoma region covered by lakes; refs 3, 9, 23)—yielding a regional flux of 3.8 Tg CH<sub>4</sub> yr<sup>-1</sup>. Using an independent mass-balance approach based on organic carbon loss from yedoma beneath thaw lakes, we estimated that decomposition of yedoma beneath Siberian lakes contributed on average 3.7 Tg CH<sub>4</sub> yr<sup>-1</sup> to the atmosphere throughout the Holocene. Given the uncertainties associated with both flux estimates (Supplementary Information), their strong correspondence supports our conclusion that North Siberian lakes are a globally significant source of atmospheric CH<sub>4</sub>.

Adding our results of ebullition from North Siberian lakes

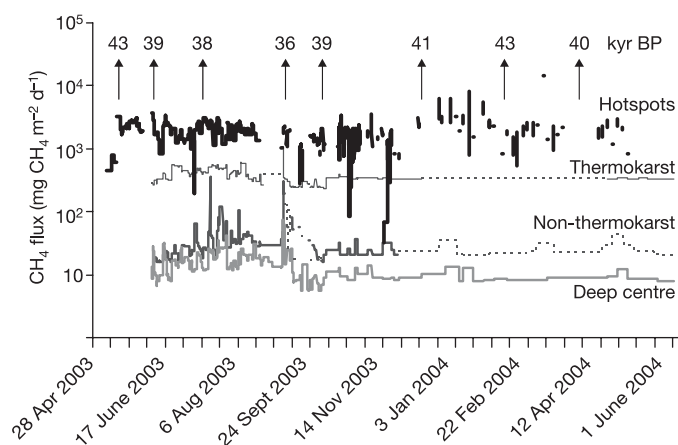


**Figure 2 | Average ebullition rates for representative areas of lakes and hotspots.** Ebullition rates along thermokarst margins (15.8 ± 2.2% of lake area) were an order of magnitude greater than ebullition rates along non-thermokarst margins (4.4 ± 1.4% of lake area) and at various depths throughout the lake centre (79.8 ± 0.8% of lake area). Hotspots (<1% of lake area) are presented here separately, and units of hotspot emission are distinct: mg CH<sub>4</sub> day<sup>-1</sup> spot<sup>-1</sup>. Ebullition from a hotspot occurs through tiny bubble tubes (<2 cm diameter) at the sediment surface, but represents CH<sub>4</sub> produced in a larger volume of lake sediments. Hotspot emissions are extrapolated by area on the basis of the number of hotspots per unit area of lake surface (Table 1). Breaks in the hotspot line are periods of no data (Supplementary Information). Numbers above hotspot data indicate the radiocarbon <sup>14</sup>C age (kyr BP) of CH<sub>4</sub> bubbles collected from a particular hotspot repeatedly throughout the study period. We interpolated fluxes (dashed lines) if fewer than 25% of the total traps were operating owing to temporary mechanical failures.

( $3.8 \text{ Tg yr}^{-1}$ ), which have not yet been included in global estimates of  $\text{CH}_4$  emissions from wetlands<sup>2,15,16,24</sup>, to a range of estimates for northern wetland flux ( $<6\text{--}40 \text{ Tg CH}_4 \text{ yr}^{-1}$ ; refs 1, 2, 4–6) increases current estimates of northern wetland  $\text{CH}_4$  emissions by 10–63%. Because yedoma lakes are only a fraction of northern lakes, ebullition measurements in other lake regions would probably further increase  $\text{CH}_4$  emission estimates.

In the zone of continuous permafrost, which comprises about half of arctic permafrost<sup>25</sup>, warming<sup>26</sup> and degradation of permafrost have caused thaw lakes to grow in number and size during recent decades<sup>27</sup>. Using GIS analysis of 1974 Multispectral Scanner (MSS) and 2000 Enhanced Thematic Mapper (ETM+) Landsat imagery, we measured a 14.7% increase in lake area (from 9.6% to 11% lakes) for a 12,000  $\text{km}^2$  territory including our study region along the Kolyma River near Cherskii, Russia (Fig. 3). This is similar to the 12% increase in lake area observed in continuous permafrost zones of West Siberia during the same period<sup>27</sup>. Applying  $\text{CH}_4$  emission rates associated with thaw margins to areas of lake expansion based on observations of hotspot distributions (see Methods), we estimated that the 14.7% increase in lake area resulted in a 58% increase in lake  $\text{CH}_4$  emissions, or  $1.4 \text{ Tg CH}_4 \text{ yr}^{-1}$  between 1974 ( $2.4 \text{ Tg CH}_4 \text{ yr}^{-1}$ ) and 2000 ( $3.8 \text{ Tg CH}_4 \text{ yr}^{-1}$ ) if extrapolated regionally. Regional warming observed during the study period<sup>28</sup> of 1974–2004 (Fig. 3) is consistent with lake expansion that contributed to rising atmospheric  $\text{CH}_4$  concentration and global temperature. This is, however, not a simple feedback loop because many processes contribute to thermokarst lake expansion and climate warming over a range of timescales.

Isotopic analyses revealed that methane collected from ebullition

in Siberian thaw lakes during 2001–2004 is of biogenic origin ( $\delta^{13}\text{C}$  of  $\text{CH}_4 = -58\text{‰}$  to  $-83\text{‰}$ ,  $\delta\text{D}$  of  $\text{CH}_4 = -338\text{‰}$  to  $-420\text{‰}$ ) (Table 1). Hotspot  $^{14}\text{C}$ , ranging from 35,260–42,900 yr (0.49–1.2% modern carbon), reflects the importance of recently thawed Pleistocene-age permafrost soils as a source of labile organic matter for methanogenesis deep within the thaw bulb of lakes (Fig. 2). Non-hotspot sources of bubbling had younger radiocarbon ages, 1,385–22,050 yr (6.4–85% modern carbon), indicating a greater influence of Holocene organic sources for methane production. Weighting the radiocarbon signature of point-source types by their abundance in lakes yielded an average annual  $^{14}\text{C}$  age of 16,520 yr, signifying that Pleistocene sediments deposited 20,000–40,000 yr ago constitute 41–83% of the  $\text{CH}_4$  emitted from Siberian lakes. The radiocarbon age of  $\text{CH}_4$  sampled from our North Siberian thaw lakes is distinct from other arctic lakes and wetlands, including the East Siberian alasses situated on sandy soils whose  $^{14}\text{C}$  of  $\text{CH}_4$  value is 95–123% modern carbon<sup>29</sup>. Therefore the unique  $^{14}\text{C}$ -depleted  $\text{CH}_4$  signature of ebullition from yedoma lakes should be considered in future studies that estimate the fraction of total atmospheric  $\text{CH}_4$  emissions derived from fossil fuels.

In conclusion, we have shown that North Siberian lakes are a significantly larger source of atmospheric  $\text{CH}_4$  than previously recognized. Emissions are dominated by ebullition, a mode of emission that we have quantified using the new technique of mapping bubbling point sources. This  $\text{CH}_4$  source is largely fuelled by thermokarst, and we have linked the expansion of thaw lakes during recent decades with a 58% increase in lake  $\text{CH}_4$  emissions, demonstrating a new feedback to climate warming. Though the recent increase in flux due to lake expansion is modest relative to

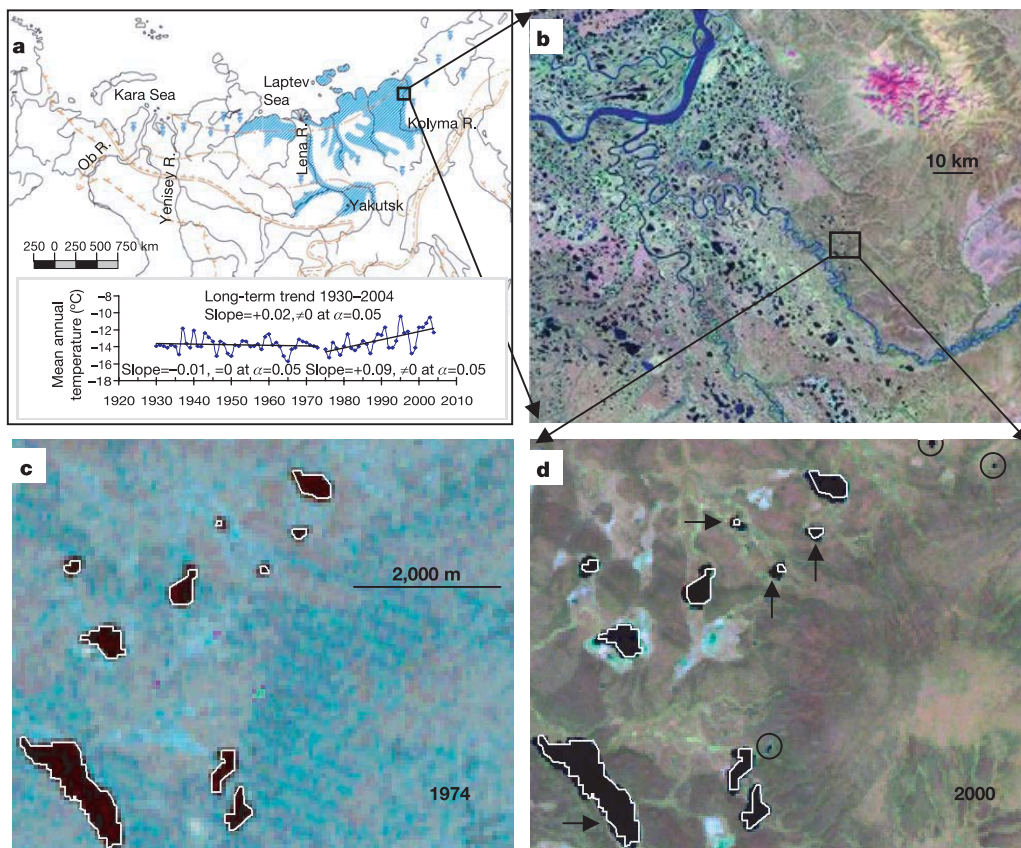


**Figure 3 | Thermokarst lake expansion.** The schematic in **a** shows yedoma distribution (blue) in North Siberia and the mean annual air temperature for the half-degree-resolution grid cell that includes our study area (box in **a** indicates location of image in **b**), interpolated from climate station records from 1930–2004 (ref. 30). Blue shading shows continuous yedoma distribution (adapted from ref. 32); blue triangles show sporadic yedoma

distribution.  $\alpha$ , significance level. The Landsat image in **b** ( $\sim 12,000 \text{ km}^2$ ) represents the region of our GIS lake change analysis from 1974 (**c**) to 2000 (**d**). The box in **b** indicates location of images in **c** and **d**. The shorelines from 1974 are delineated as white polygons, while some areas of expansion of thaw lakes are indicated by arrows and formation of new lakes by circles on the 2000 image in **d**.

anthropogenic emissions<sup>1,2,7</sup>, the ~500 Gt of labile Pleistocene-aged C in ice-rich yedoma permafrost<sup>11</sup> could greatly intensify the positive feedback to high-latitude warming by releasing tens of thousands of teragrams of CH<sub>4</sub> through ebullition from thermokarst lakes if northeast Siberia continues to warm in the future, as projected<sup>26</sup>.

## METHODS

All numbers following a ± sign are standard deviations unless otherwise noted. Equations were developed to extrapolate flux measurements to whole lake and regional emission estimates (Supplementary Information).

**Ebullition measured by bubble traps.** We captured ebullition continuously using umbrella-shaped floating bubble traps (~1-m diameter, 25 traps randomly placed for background ebullition, 16 traps fixed over point sources and hotspots of bubbling) with daily measurements of bubble volume from April 26, 2003 through June 1, 2004 at two lakes (maximum depths 16.5 m and 11 m, with areas 0.11 km<sup>2</sup> and 0.06 km<sup>2</sup>) near the Northeast Science Station in Cherskii (68° 45' 36" N, 161° 20' 34" E). Gas concentrations and isotopes were also measured (Supplementary Information). To verify that our intensively studied lakes were regionally representative of thermokarst lakes on yedoma territory, we made ground surveys of 35 other lakes and took aerial photographs of 60 lakes in Northern Siberia.

Stable isotope compositions are expressed in δ (‰) = 10<sup>3</sup> ((R<sub>sample</sub>/R<sub>standard</sub>) - 1), where R is <sup>13</sup>C/<sup>12</sup>C or D/H and standards refer to the Vienna Pee Dee belemnite (VPDB) and Vienna standard mean ocean water (VSMOW), respectively. The analytical errors of the stable isotopic analyses are ±0.1‰ for δ<sup>13</sup>C and ±0.1‰ for δD. We express radiocarbon data as the percentage of modern carbon, ((<sup>14</sup>C/<sup>12</sup>C)<sub>sample</sub>/(<sup>14</sup>C/<sup>12</sup>C)<sub>standard</sub>) × 100, which is the percentage of <sup>14</sup>C/<sup>12</sup>C ratio normalized to δ<sup>13</sup>C = -25‰ and decay-corrected relative to that of an oxalic standard in 1950 (ref. 30).

**Mapping bubble clusters in lake ice as 'point sources' of ebullition.** We removed snow from lake surfaces along six 50 m × 1 m transects per lake (Fig. 1) in early winter to count the number and type of bubble clusters in lake ice that represent 'point sources' of ebullition. We categorized four types of bubble patterns in lake ice and measured winter CH<sub>4</sub> flux rates (mg CH<sub>4</sub> day<sup>-1</sup> per point) associated with each 'point-source' category and hotspots using floating traps under the ice (Supplementary Information). Average emissions from point sources and hotspots were extrapolated to entire lakes based on transects of bubble-cluster and hotspot densities in ice over shallow, medium and deep water depths in thermokarst and non-thermokarst areas of lakes. We include the estimated flux from point sources in addition to the randomly placed bubble trap flux (background ebullition) because the probability of capturing point sources and hotspots in randomly placed traps was 0.001% and there was no overlap between values of point-source fluxes and values of background ebullition.

**Mass-balance approach to Holocene lake emissions.** To assess the plausibility of our CH<sub>4</sub> flux estimate of 3.8 Tg CH<sub>4</sub> yr<sup>-1</sup> we used an independent mass-balance approach based on Holocene carbon loss associated with thermokarst lake development. The mean carbon content of decomposed yedoma beneath two former thermokarst lakes (18.0 ± 1.4 kg C m<sup>-3</sup>, standard error of 15 samples) is 33% less than in undisturbed yedoma (26.8 ± 1.5 kg C m<sup>-3</sup>, standard error of 54 samples). We assumed half of this carbon was converted to CH<sub>4</sub>, on the basis of the stoichiometry of methane production from cellulose degradation<sup>31</sup>. Applying this 16.5% carbon loss due to methanogenesis beneath lakes to yedoma territory of North Siberia (1 × 10<sup>6</sup> km<sup>2</sup>, 25 m average thickness, 50% ice content)<sup>3,10,23</sup>, which has been degraded by migratory lakes whose scars cover 50% of the region<sup>23</sup>, yields a release of 28 Gt C from CH<sub>4</sub> during the Holocene (10,000 yr) or on average, 3.7 Tg CH<sub>4</sub> yr<sup>-1</sup>. This estimate is conservative because it does not include CH<sub>4</sub> derived from Holocene-age lake deposits.

Future CH<sub>4</sub> release via ebullition from expanding thaw lakes in the yedoma region is estimated to be of the order of tens of thousands of teragrams based on the amount of labile carbon remaining in yedoma permafrost (500 Gt; ref. 11) and the proportion of carbon converted to CH<sub>4</sub> during methanogenesis (16.5%).

**Estimating CH<sub>4</sub> fluxes from expanding lakes.** The years of the images analysed had temperature and precipitation values typical of the twentieth century for our study region<sup>28</sup>. We assumed flux rates for lakes in 1974 were the same as current rates of our two intensive study lakes (24.9 g CH<sub>4</sub> m<sup>-2</sup> yr<sup>-1</sup>). Applying this modest rate to 50% of the region's lakes in 2000 and higher rates (43.7 g CH<sub>4</sub> m<sup>-2</sup> yr<sup>-1</sup>) to the other half of the region's lakes, where intense erosion has led to the observed 14.7% increase in lake area, resulted in a 58% increase in lake CH<sub>4</sub> emissions. Extrapolating CH<sub>4</sub> fluxes associated with lake expansion to the yedoma region yields an estimated increase in lake emissions of 1.4 Tg CH<sub>4</sub> yr<sup>-1</sup> between 1974 (2.4 Tg CH<sub>4</sub> yr<sup>-1</sup>) and 2000 (3.8 Tg CH<sub>4</sub> yr<sup>-1</sup>).

Received 5 December 2005; accepted 3 July 2006.

1. Intergovernmental Panel on Climate Change (IPCC), *The Scientific Basis* (Cambridge Univ. Press, New York, 2001).
2. Mikaloff Fletcher, S. E., Tans, P. P., Bruhwiler, L. M., Miller, J. B. & Heimann, M. CH<sub>4</sub> source estimated from atmospheric observations of CH<sub>4</sub> and its <sup>13</sup>C/<sup>12</sup>C isotopic ratios: 1. Inverse modelling of source processes. *Glob. Biogeochem. Cycles* **18**, GB4004, doi:10.1029/2004GB002223 (2004).
3. Zimov, S. A. et al. North Siberian lakes: A methane source fuelled by Pleistocene carbon. *Science* **277**, 800–802 (1997).
4. Roulet, N. T. et al. Role of Hudson Bay lowland as a source of atmospheric methane. *J. Geophys. Res.* **99**, 1439–1454 (1994).
5. Reeburgh, W. S. et al. A CH<sub>4</sub> emission estimate for the Kuparuk River basin, Alaska. *J. Geophys. Res.* **103**, 29005–29013 (1998).
6. Worthy, D. E., Levin, J. I., Hopper, F., Ernst, M. K. & Trivett, N. B. A. Evidence for a link between climate and northern wetland methane emissions. *J. Geophys. Res.* **105**, 4031–4038 (2000).
7. Fung, I. et al. Three-dimensional model synthesis of the global methane cycle. *J. Geophys. Res.* **96**, 13033–13065 (1991).
8. Dlugokencky, E. J., Masarie, K. A., Lang, P. M. & Tans, P. P. Continuing decline in the growth rate of the atmospheric methane burden. *Nature* **393**, 447–450 (1998).
9. Mostakhov, S. E. in *Mezhdunarodnaia konferentsiia po merzlotovedeniui, Podzemnye vody kriolitofery* (ed. Tolstikhin, N. I.) (Iakustkoe Knizhnoe Izdatel'stvo, Iakutsk, Russia, 1973).
10. Romanovskii, N. N. et al. Thermokarst and land-ocean interactions, Laptev Sea Region, Russia. *Perm. Periglac. Process.* **11**, 137–152 (2002).
11. Zimov, S. A., Schuur, E. A. G. & Chapin, F. S. III Permafrost and the global carbon budget. *Science* **312**, 1612–1613 (2006).
12. Keller, M. & Stallard, R. F. Methane emission by bubbling from Gatun Lake, Panama. *J. Geophys. Res.* **99**, 8307–8319 (1994).
13. Casper, P., Maberly, S. C., Hall, G. H. & Finlay, B. J. Fluxes of methane and carbon dioxide from a small productive lake to the atmosphere. *Biogeochemistry* **49**, 1–19 (2000).
14. Kling, G., Kipphut, G. W. & Miller, M. C. The flux of CO<sub>2</sub> and CH<sub>4</sub> from lakes and rivers in arctic Alaska. *Hydrobiologia* **240**, 23–36 (1992).
15. Mathews, E. & Fung, I. Methane emission from natural wetlands: Global distribution, area, and environmental characteristics of sources. *Glob. Biogeochem. Cycles* **1**, 61–86 (1987).
16. Aselmann, I. & Crutzen, P. J. Global distribution of natural freshwater wetlands, rice paddies, their net primary productivity, seasonality, and possible methane emissions. *J. Atmos. Chem.* **8**, 307–358 (1989).
17. Phelps, A. R., Peterson, K. M. & Jeffries, M. O. Methane efflux from high-latitude lakes during spring ice melt. *J. Geophys. Res.* **103**, 29029–29036 (1998).
18. Bartlett, K. B., Crill, P. M., Sass, R. L., Harriss, R. C. & Dise, N. B. Methane emissions from tundra environments in the Yukon-Kuskokwim Delta, Alaska. *J. Geophys. Res.* **97**, 16645–16660 (1992).
19. Roulet, N. T., Crill, P. M., Comer, N. T., Dove, A. & Boubonniere, R. A. CO<sub>2</sub> and CH<sub>4</sub> flux between a boreal beaver pond and the atmosphere. *J. Geophys. Res.* **102**, 29313–29319 (1997).
20. Nakayama, T. Estimation of Methane Emission from Natural Wetlands in Siberian Permafrost Area. 1–100, PhD dissertation, Hokkaido Univ. (1995).
21. Corradi, C., Kolle, O., Walter, K., Zimov, S. A. & Schulze, E.-D. Carbon dioxide and methane exchange of a north-east Siberian tussock tundra. *Glob. Change Biol.* **11**, 1910–1925 (2005).
22. Bastviken, D., Cole, J., Pace, M. & Tranvik, L. Methane emissions from lakes: Dependence of lake characteristics, two regional assessments, and a global estimate. *Glob. Biogeochem. Cycles* **18**, GB3010, doi:10.1029/2004GB002238 (2004).
23. Czudek, T. & Demek, J. Thermokarst in Siberia and its influence on the development of lowland relief. *Quat. Res.* **1**, 103–120 (1970).
24. Zhuang, Q. et al. Methane fluxes between terrestrial ecosystems and the atmosphere at northern high latitudes during the past century: A retrospective analysis with a process-based biogeochemistry model. *Glob. Biogeochem. Cycles* **18**, GB3010, doi:10.1029/2004GB002239 (2004).
25. Brown, J., Ferrians, O. J. Jr, Heginbottom, J. A. & Melnikov, E. S. *Circum-Arctic Map of Permafrost and Ground-Ice Conditions* 1:10,000,000 (US Geological Survey Circum-Pacific Map CP-45, Reston, Virginia, 1997).
26. Sazonova, T. S., Romanovsky, V. E., Walsh, J. E. & Sergueev, D. O. Permafrost dynamics in the 20th and 21st centuries along the East Siberian transect. *J. Geophys. Res.* **109**, doi:10.1029/2003JD003680 (2004).
27. Smith, L. C., Sheng, Y., MacDonald, G. M. & Hinzman, L. D. Disappearing arctic lakes. *Science* **308**, 1429 (2005).
28. Willmott, C. J., & Matsuura, K. *Arctic Terrestrial Air Temperature and Precipitation Monthly and Annual Time Series (1930–2000)* Version 1 (Univ. Delaware); (<http://climate.geog.udel.edu/~climate/>) or (<http://rims.unh.edu/data/data.cgi>).
29. Nakagawa, F., Yoshida, N., Nojiri, Y. & Makarov, V. N. Production of methane from alasses in eastern Siberia: Implications from its <sup>14</sup>C and stable isotope compositions. *Global Biogeochem. Cycles* **16**, doi:10.1029/2000GB001384 (2002).

30. Stuiver, M. M. & Polach, H. Reporting of  $^{14}\text{C}$  data. *Radiocarbon* **19**, 355–363 (1977).
31. Conrad, R., Klose, M. & Clause, P. Pathway of  $\text{CH}_4$  formation in anoxic rice field soil and rice roots determined by  $^{13}\text{C}$ -stable isotope fractionation. *Chemosphere* **47**, 797–806 (2002).
32. Romanovsky, N. N. *Osnovy Kriogeneza Litosfery* (Izdatelstvo Moscow State University, Moscow, 1993).

**Supplementary Information** is linked to the online version of the paper at [www.nature.com/nature](http://www.nature.com/nature).

**Acknowledgements** We thank S. P. Davidov and D. A. Draluk for contributions to the research; D. Nidzgorski and E. Carr for field assistance; the Northeast Science Station for logistic support; K. Dutta, T. Schuur and the University of Florida for helping to prepare the radiocarbon targets; S. Marchenko and V. Romanovskii for assistance in analysing Cherskii climate records; and E. Dlugokencky, J. Hobbie, T. Schuur, D. Valentine, and M. S. Bret-Harte for constructive reviews. Research funding was provided by the National Science

Foundation through the Russian-American Initiative on Shelf-Land Environments of the Arctic (RAISE) of the Arctic System Science programme (ARCSS) and Polar Programs, the Environmental Protection Agency STAR Fellowship programme, and the NASA Earth System Science Fellowship programme.

**Author Contributions** K.M.W. was the primary investigator in this study, responsible for study design, field work, laboratory measurements, GIS and isotope analyses, data analysis, interpretation and writing. S.A.Z. and F.S.C. contributed to project planning, experimental work, and interpretation of results. J.P.C. assisted with isotope analyses and interpretation. D.V. contributed to the study design and interpretation of the GIS analysis of lake area change. All co-authors provided constructive comments on the manuscript.

**Author Information** Reprints and permissions information is available at [www.nature.com/reprints](http://www.nature.com/reprints). The authors declare no competing financial interests. Correspondence and requests for materials should be addressed to K.M.W. ([ftkmw1@uaf.edu](mailto:ftkmw1@uaf.edu)).